Binding Energies of Ag^+ and Cd^+ Complexes from Analysis of Radiative Association Kinetics

Yen-Peng Ho, Yu-Chuan Yang, Stephen J. Klippenstein,*,† and Robert C. Dunbar*

Chemistry Department, Case Western Reserve University, Cleveland, Ohio 44106

Received: November 8, 1996; In Final Form: February 24, 1997[⊗]

Association reactions of Cd^+ with benzene and of Ag^+ with acetone and several unsaturated hydrocarbons were observed in the Fourier-transform ion cyclotron resonance (FT-ICR) spectrometer. The reactions were presumed to occur by radiative association (RA) involving infrared photon emission, and the kinetics were analyzed to derive bond strengths for the ion−neutral complexes. To supply the structures, infrared frequencies, and infrared intensities required for this analysis, *ab initio* calculations at the Hartree−Fock (HF) and second-order Moeller−Plesset perturbation theory (MP2) levels were carried out for the reactants and the association complexes, and the results are reported. The RA kinetics analysis yielded values for the binding energies of 1.41 ± 0.2 eV for Cd^+(benzene), 1.68 ± 0.2 eV for Ag^+(benzene), 1.66 ± 0.2 eV for Ag^+(acetone), 1.70 ± 0.2 eV for Ag^+(isoprene), and 1.71 ± 0.2 eV for Ag^+(2-pentene). The MP2-derived modeling gave higher (and more reliable) binding energies than the HF-derived modeling, but the HF-level modeling was found to provide estimates of useful precision, except for the Ag^+(benzene) case. Binding energies were also estimated for the observed Ag^+L_2 complexes, and within experimental and modeling error the second ligand was found to bind with the same energy as the first. Clustering of six or more acetaldehydes with Ag^+ was observed, but it was considered most likely that this reflected fast association with low-abundance polymeric impurities in the acetaldehyde sample.

Introduction

Stimulated by the rapid development of techniques for preparing a wide variety of stable coordinatively unsaturated species in the gas phase,[1−4] recent interest has expanded in characterizing and understanding the bonding in "exotic" organometallic complexes. The chemical simplicity of the low-pressure gas-phase environment and the possibility of separating solvent effects from intrinsic bonding thermochemistry have been key factors in making this a rewarding new area of metal ion chemistry. Established techniques for determining ligand−metal bond strengths include ligand exchange equilibrium,[5,6] bracketing by exothermic ion−neutral reactions,[1] metastable ion dissociation,[7] collision-induced dissociation,[8−12] and photodissociation methods,[13−17] as well as Hess's law calculations from independently determined thermochemical data.[1]

A recent, promising addition to this array of tools is the kinetic analysis of radiative association reactions (the RA kinetics approach).[18−23] The sensitive dependence of the rates of such reactions to the binding energy makes this an approach with high potential precision, and careful application to several systems has suggested that in fact its accuracy can be competitive with other approaches. We apply this approach here to the determination of several metal−ligand binding energies. One of the best aspects of this approach is that it is complementary to other methods (e.g., dissociative ionization thresholds, CID thresholds, photodissociation thresholds, the "kinetic method") which are based on observing the dissociation of the complex of interest. The radiative association approach observes the association of separate reactants to give the complex and in correlation with dissociation measurements should give a revealing view of such difficult-to-characterize complications as barriers in the reaction path and intracomplex rearrangements and insertions.

RA kinetic analysis derives the binding energy which is consistent with the observed rate constant for the association process

$$M^+ + L \xrightarrow{k_2} [ML]^+ \qquad (1)$$

where k_2 is the apparent bimolecular rate constant defined as $-\mathrm{d}\ \ln[M^+]/\mathrm{d}t$ divided by the neutral density. Figure 1 shows a schematic potential energy plot along the reaction coordinate for this process.

To understand the relation between binding energy and the association process, we may picture that a metal ion M^+ collides with a neutral ligand L to form an activated metastable adduct, $[ML^+]^*$. This activated complex has an initial internal energy equal to the sum of a thermal energy E_{thermal} and the dissociation energy E_0. The thermal energy, E_{thermal}, comes from the internal energies of reactants plus translational energy dissipated into internal degrees of freedom of the activated complex during the formation of the complex. The metastable adduct may redissociate back to the reactants or be stabilized by energy loss processes, and the kinetics of this competition is highly sensitive to the binding energy.

A more detailed picture is frequently given in terms of the kinetic scheme

$$M^+ + L \underset{k_b}{\overset{k_f}{\rightleftharpoons}} (ML)^{+\bullet} \xrightarrow{k_r} (ML)^+ + h\nu \qquad (2)$$

$$(ML)^{+\bullet} \xrightarrow{k_c[B]} (ML)^+$$

where k_f, k_b, k_r, and k_c stand for complex formation rate constant, complex redissociation rate constant, radiative stabilization rate constant, and collisional stabilization rate constant, respectively. In this scheme the complex stabilization is achieved either by

* Authors to whom correspondence should be addressed.

† Present address: Theoretical Chemistry Group, Chemistry Division, Argonne National Laboratory, Argonne, IL 60439.

[⊗] Abstract published in *Advance ACS Abstracts,* April 1, 1997.

S1089-5639(96)03728-0 CCC: $14.00

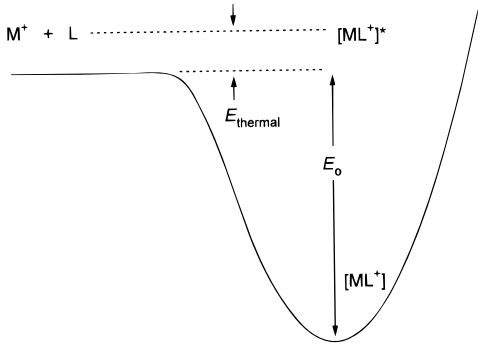

Figure 1. Energy diagram for the association process.

IR radiative emission (k_r) or by collisional energy transfer (k_c) through an ion−neutral collision with a bath gas molecule B. However, it is the radiative association channel (k_r) which has been the focus of recent attention and analysis for quantitative bond strength determinations. Except for the pressure dependence experiments, the present work was all carried out at pressures sufficiently low that the collisional association channel was unimportant and could be ignored in the analysis (*vide infra*).

Many binding energies of complexes of first-row transition metal ions with various ligands have been measured by different methods.[1−4] There has been less study of second- and third-row transition metal ion complexes. In this work, the reactions of Cd^+ with benzene and Ag^+ with benzene, isoprene, 2-pentene, acetone, and acetaldehyde were studied, and RA kinetic analysis was applied to derive binding energies. For the M^+L complexes the data were analyzed using the most complete and accurate available theoretical approach, based on detailed RRKM evaluations employing parameters determined from *ab initio* calculations.[23] Several Ag^+L_2 complexes were also studied, for which it was only feasible to carry out the RA kinetics analysis using either the more approximate standard hydrocarbon approach or extrapolations from the single ligand quantum chemical data.

Experimental Part

The association reactions of Ag^+ with acetone and acetaldehyde were studied at the National High Magnetic Field Lab in Tallahassee, FL. Data were acquired there with an Extrel FTMS-2000 Fourier-transform ion cyclotron resonance mass spectrometer equipped with a 3 T superconducting magnet, 1.875 in. cubic traps in a standard dual trap configuration, and an Odyssey data system. The silver ions were produced by focusing the laser light pulse from the doubled output of a Continuum Nd:YAG laser on a thin silver plate which was mounted on the automatic insertion probe. Both the reaction and detection were carried out using the same trap of the dual cell. The cell temperatures in the temperature dependence experiments for the reaction of Ag^+ with acetone were determined using the thermocouple attached to the can surface near the source region.

The rest of the experiments were carried out using the Fourier-transform ion cyclotron resonance mass spectrometer in the CWRU laboratory, equipped with an IonSpec data system. The ions were trapped in a 1 in. cubical cell at a magnetic field of 1.4 T. The metal ions were produced by focusing the 532 nm light pulse (generated by a Nd:YAG laser) onto a metal plate attached to a sample holder near the cell.

The intensities of metal ion and ion complex were monitored as a function of reaction time to derive the association rate constant. Several time plots for the association reactions are

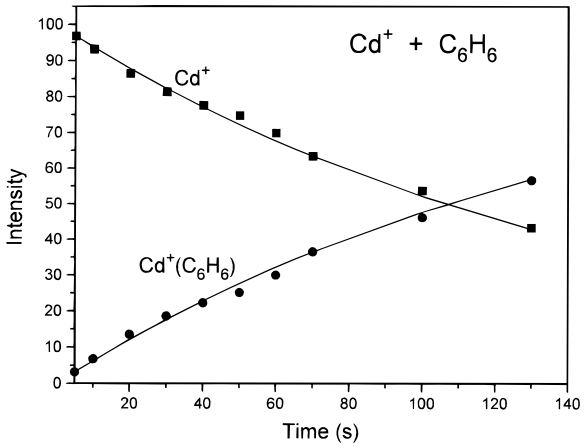

Figure 2. Association reaction of Cd^+ with benzene at 300 K and a pressure of 4×10^{-8} Torr.

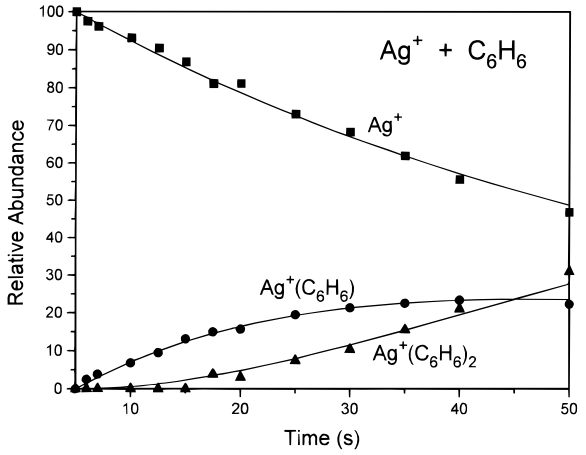

Figure 3. Association reaction of Ag^+ with benzene at 300 K and a pressure of 2×10^{-8} Torr.

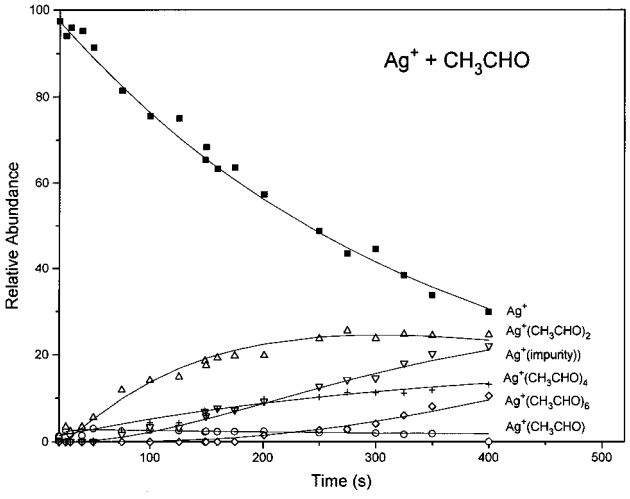

Figure 4. Association reaction of Ag^+ with acetaldehyde at 294 K and a pressure of 1.4×10^{-7} Torr.

illustrated in Figures 2−4. Since the metal ions produced by laser desorption were hot in the beginning, initially they either did not react or reacted slower than the thermalized ions did. Therefore, the reaction rate constant varied during the thermalization period. After the metal ions were thermalized through collision with the neutral reactant and emission of photons, the reaction followed a pseudo-first-order rate law. The fits to first-order kinetics shown in Figures 2−4 were accordingly made to data points at times after the initial nonthermal behavior had

died away, and only this portion of the data is displayed in the figures.

The neutral pressures of benzene, pentene, and isoprene were read from current of an ion pump. The ion pump was previously calibrated for benzene against a Bayard-Alpert gauge and may be uncertain by a factor of 1.5. For the other two neutrals, experience suggests that the absolute pressures may be uncertain by a factor of 2.

For acetone (studied in the Tallahassee lab), the known proton transfer reaction

$$CH_3CO^+ + (CH_3)_2CO \rightarrow (CH_3)_2COH^+ + CH_2CO \quad (3)$$

with a reaction rate of 2.0×10^{-10} cm^3 molecule^{-1} s^{-1} was used for pressure calibration.[24] The ratio of true acetone pressure to gauge pressure was determined by measuring the apparent disappearance rate constant of CH_3CO^+ via the reaction of eq 3 based on the ion gauge pressure reading and comparing this with the known true rate constant.

For acetaldehyde (studied in the Tallahassee lab), a well-known reaction rate constant was not found for pressure calibration. The same gauge calibration used for acetone was also used for acetaldehyde, corrected by the fact that the ion gauge sensitivity for acetaldehyde is lower than for acetone by a factor of 1.95/2.50.[25]

The neutral pressures were 2×10^{-8} Torr for the hydrocarbons reacting with Ag^+, 4×10^{-8} Torr for benzene reacting with Cd^+, 7×10^{-8} Torr for acetone, and 14×10^{-8} Torr for acetaldehyde. Comparing the corresponding ion−neutral orbiting collision rates with the k_r values assigned below (Table 2), it is seen that collisional quenching would contribute less than 15% of the overall relaxation in all cases. Thus, the error in neglecting collisional quenching contributions is small compared with other sources of uncertainty. For the pressure dependence experiments the pressure ranged up to $\sim 1 \times 10^{-6}$ Torr.

Acetaldehyde forms a cyclic trimer and a cyclic tetramer under acid catalysis. Since a variety of polymerization product ions were observed in the association experiments described here, it was important to consider the possible presence of polymerized neutral molecules in the neutral sample gas. An NMR spectrum of the sample was acquired, which showed no trimers, tetramers, or other impurities within the detection limits (which we estimate to be ~0.1%). Combined with the discrimination against polymeric material occurring during sample vaporization, it was hoped that this would provide sufficient assurance that acetaldehyde monomer was the only significant reactant neutral in the ICR cell. As discussed below, this may not have been the case in reality.

Theory

Kinetic Modeling. Following the formulation of Kofel and McMahon,[26] most estimates of complex binding energies from the kinetic analysis of association results[18−21] have been based on the assumption that all the microscopic rates in eq 2, such as IR emission rates and redissociation rates, are single values. In fact, these microscopic rates are energy E-dependent and angular momentum J-dependent quantities which deviate substantially from any single value since the distributions of these quantities in the initially formed complexes are quite broad.

In recent work we described a generalized formalism that takes into account the distribution of internal energies and angular momenta of the complexes arising from the thermal distribution of reactants.[22,23] This approach was employed in the present work to model the reactions of metal ions with organic ligands and to derive the binding energies for the complexes. A brief summary of the key equations is given here, while more detail can be found in ref 23. In this approach, k_f and k_b are evaluated according to transition state theory for the specific case of a long-range ion-induced-dipole plus ion-dipole potential. The apparent bimolecular rate constant is written as a thermal average of the product of the complex formation rate constant with the stabilization efficiency $\Phi(E,J)$:

$$k_2 = \int \mathrm{d}E\, \mathrm{d}J\, P_{\mathrm{reactants}}(E,J) k_f(E,J)\, \Phi(E,J) \quad (4)$$

where

$$\Phi(E,J) = \frac{k_r(E,J) + k_c(E,J)[\mathrm{L}]}{k_d(E,J) + k_r(E,J) + k_c(E,J)[\mathrm{L}]} \quad (5)$$

In eq 4 $P_{\mathrm{reactants}}(E,J)$ is the probability for reactants to have specific energy E and total angular momentum J and is given by

$$P_{\mathrm{reactants}}(E,J) = \frac{\rho_{E,J}^{\mathrm{reactants}} \exp(-E/kT)}{Q_{\mathrm{reactants}}(T)} \quad (6)$$

where $Q_{\mathrm{reactants}}(T)$ is the partition function for reactants and $\rho_{E,J}^{\mathrm{reactants}}$ is the density of states for the reactant. The formation rate constant k_f and redissociation rate constant k_b are given in terms of the transition state number of states $N_{EJ}^{\ddagger}$ and the density of states ρ_{EJ} for reactants and complex:

$$k_f(E,J) = N_{EJ}^{\ddagger}/h\rho_{E,J}^{\mathrm{reactants}} \quad (7)$$

$$k_b(E,J) = N_{EJ}^{\ddagger}/h\rho_{E,J}^{\mathrm{complex}} \quad (8)$$

where h is Planck's constant.

Combining eqs 4−7 gives the general expression for the association rate constant,

$$k_2 = \frac{1}{hQ_{\mathrm{reactants}}} \int \mathrm{d}E\, \mathrm{d}J\, N_{EJ} \times \exp(-E/kT) \left\{ \frac{k_r(E,J) + k_c(E,J)[\mathrm{L}]}{k_d(E,J) + k_r(E,J) + k_c(E,J)[\mathrm{L}]} \right\} \quad (9)$$

We can fit this predicted association rate constant to the experimental results by varying the assumed binding energy for the complex. Although it is not possible to carry out the experiments with absolute zero pressure, the low-pressure conditions of the present experiments assured that the collisional contributions to the total association rate constants were unimportant (the modeling suggests contributions of about 15% or less), permitting the simplification of neglecting the k_c terms in the equations. The rate constant in this limit of low pressure is labeled here as k_{ra}.

The radiative rate constant k_r required in the calculation of k_{ra} can be obtained from (1) radiative cooling rate experiments,[27,28] (2) quantum chemical calculations,[29] or (3) a pressure-dependent plot of association rate constants.[30] The present analyses used calculated values following approach 2, although the results were confirmed for the Ag^+/benzene case by the supplementary application of approach 3 as described below. As has been described,[23] approach 2 employs quantum chemical values of IR absorption frequencies and intensities to calculate k_r from the basic equation[31]

$$k_r\,(\mathrm{s}^{-1}) = \sum_i \sum_n 1.25 \times 10^{-7} n \nu_i^2(\mathrm{cm}^{-1}) I_i\,(\mathrm{km/mol}) P_i(n) \quad (10)$$

TABLE 1: Kinetics Data for Metal Ion/Molecule Reactions

reactants	product	assocn rate constant (cm^3 $molecule^{-1}$ s^{-1})	neutral press. (Torr)	temp (K)
Cd^+, benzene	$Cd(benzene)^+$	3.9×10^{-12}	4.0×10^{-8}	300
Ag^+, benzene	$Ag(benzene)^+$	2.41×10^{-11}	2.0×10^{-8}	300
$Ag(benzene)^+$, benzene	$Ag(benzene)_2^+$	5.37×10^{-11}	2.0×10^{-8}	300
Ag^+, isoprene	$Ag(isoprene)^+$	3.79×10^{-11}	2.0×10^{-8}	300
$Ag(isoprene)^+$, isoprene	$Ag(isoprene)_2^+$	5.51×10^{-11}	2.0×10^{-8}	300
Ag^+, 2-pentene	$Ag(2\text{-pentene})^+$	3.84×10^{-11}	2.0×10^{-8}	300
$Ag(2\text{-pentene})^+$, 2-pentene	$Ag(2\text{-pentene})_2^+$	6.45×10^{-11}	2.0×10^{-8}	300
Ag^+, acetone	$Ag^+(acetone)$	7.9×10^{-12}	6.9×10^{-8}	294
$Ag^+(acetone)$, acetone	$Ag^+(acetone)_2$	8.8×10^{-11}	6.9×10^{-8}	294
Ag^+, acetaldehyde[a]	$Ag^+(acetaldehyde)$	5.5×10^{-13}	1.4×10^{-7}	294

[a] Rate constant assuming monomer acetaldehyde reactant. See text.

where υ_i is the frequency of mode *i*, *n* is the vibration level for each mode, I_i is the IR intensity, and $P_i(n)$, which is a microcanonical distribution function, is the probability of occupying the *n*th level of vibrational mode *i*. For the present systems, the IR frequencies and intensities for the complexes were available from the *ab initio* calculations.

As in other studies,[18−23] this approach to assigning k_r requires the assumption that a single IR photon emission from the metastable complex results in a stabilized complex. The validity of this assumption hinges on the notion that emission of an IR photon with even a few hundred cm^{-1} results in such a large reduction in the redissociation rate that the probability of a subsequent dissociation of the complex becomes negligible. This notion is valid for the complexes of modest size of interest here, although it is certainly not good for larger complexes with hundreds of internal degrees of freedom. Note, however, that in such instances it should still be possible to model the kinetics accurately with a similar set of parameters by resorting to master equation simulations.

Quantum Chemical Methodology. The vibrational frequencies, molecular structures, and IR absorption intensities required for the modeling were obtained on the basis of *ab initio* quantum chemical simulations employing the GAUSSIAN 92 and 94 software packages.[32,33] The standard 6-31G* basis set with pure d functions was generally employed for the ligands.[34] The Ag basis set developed by Langhoff *et al.*,[35] which combines the relativistic effective core potential of Hay and Wadt[36] with a (6s6p5d3f)/[5s4p4d1f] set for the valence plus polarization basis, was employed here with one modification. In particular, the GAUSSIAN software does not allow for frequency evaluations with f functions, and so these functions were not included in the present Ag basis. A similar basis did not appear to be available for Cd, and so the smaller LANL2DZ basis was instead employed.[33] This basis set combines the Hay and Wadt relativistic effective core potential[36] with a double-zeta description of the valence space.[37]

The geometries were optimized at the Hartree−Fock (HF)[34,38] and second-order Moeller−Plesset perturbation theory (MP2)[39,40] levels employing analytic derivatives. The vibrational frequencies and IR absorption intensities were estimated via numerical differentiation of the analytic first derivatives at these same levels of theory. It is perhaps worth noting that for standard organic species the intensities are typically accurate to within about a factor of 2 at the HF/6-31G* level[41] and a factor of 1.5 at the MP2/6-31G* level.[42] The results of these quantum chemical evaluations are summarized in the Appendix and the Supporting Information. The MP2 based modeling results are expected to provide the most meaningful estimates for the binding energy and will thus be the focus of the following discussions. However, the HF-based modeling results will also be presented since they are indicative of the kind of accuracy one can obtain with more limited computational effort.

For transition metal-containing species such single-reference-based methods are often very inaccurate. However, for the Ag^+-(d^{10}) and Cd^+($d^{10}s$) cations of interest here the lowest lying excited electronic states are well separated from the ground state (i.e., by approximately 5 eV). As a result, HF and MP2 methodologies should provide reasonably realistic results for the frequencies, intensities, and molecular structures of these metal/ligand cationic complexes. Meanwhile, the absolute values of the quantum chemical binding energies, which might be still be expected to be somewhat inaccurate, are of no importance to the modeling.

Density functional theory (DFT) provides another relatively easily implemented quantum chemical methodology for estimating molecular structures and IR properties. Unfortunately, its implementation at the B3LYP[43] level with the GAUSSIAN software led to numerical instabilities in the optimization of the geometries for the present complexes. Such calculations were thus not considered further here.

Results

Association Reaction Rates. The reactants and products of the association reactions are listed in Table 1. No product beyond $Cd(C_6H_6)^+$ was observed for the reaction of Cd^+ with benzene after a reaction time of 130 s at 4×10^{-8} Torr (roughly 200 ion−neutral collisions). For the associations of Ag^+ with organic molecules, all except the reaction with acetaldehyde gave successively the monomer complex and the dimer complex with no further association steps or side products. A series of products were observed for the association of Ag^+ with acetaldehyde. For illustration, plots of the metal ion and product ion abundances vs time are shown in Figures 2−4. The solid curve in Figure 2 is a fit of the data to a pseudo-first-order rate law. When sequential products were observed as seen in Figures 3 and 4, the data were fitted to a sequential reaction kinetic scheme.

In the case of association of Ag^+ with acetaldehyde, sequential products from monomer to hexamer complexes, along with unidentified ions at *m*/*z* 209 and 211, presumed to be impurity products, were observed. Trimer and pentamer complexes were only observed in some spectra, and their abundances were barely above the noise level. As shown in Figure 4, the observed evolution of products could be fitted very well to a kinetic scheme assuming successive additions of acetaldehyde monomers to the complex, starting with bare Ag^+. The peaks at *m*/*z* 209 and 211 were assumed to arise from reaction of Ag^+ with unidentified contaminants.

The association rate constants for the reactions studied are given in Table 1 where the neutral pressures and reaction temperatures are also indicated.

Pressure Dependence and Radiative Rate Constants. Calculated k_r values are reported in Table 2 for the *E* and *J*

TABLE 2: Binding Energies and Radiative Rates Derived from the *ab Initio* Calculations

complex	*ab initio* binding energy (eV)[a]	radiative rate k_r from *ab initio* results (s^{-1})[b]
Cd^+(benzene)	1.57	11
Ag^+(benzene)	1.73 (1.18)	10
Ag^+(isoprene)	1.69 (1.18)	19
Ag^+(2-pentene)	1.68 (1.10)[c]	11[c]
Ag^+(acetone)	1.70 (1.47)	37
Ag^+(acetaldehyde)	1.53 (1.34)	61

[a] The primary results are the MP2 values while those in parentheses are the HF results. The former estimates typically have an uncertainty of about 0.2−0.5 eV while the latter are even more uncertain. [b] Radiative rate for a complex formed from reactants having internal energy and total angular momentum corresponding to the midpoints of the *E* and *J* integrals in eq 9. The MP2 estimates for the IR frequencies and intensities are employed in each instance. [c] The MP2 estimates for this species had one imaginary frequency corresponding to a torsional mode of the complex, and thus the binding energy is an upper bound within the MP2 model. The radiative rate constant and other aspects of the modeling were approximately corrected for this imaginary frequency as discussed in the Supporting Information.

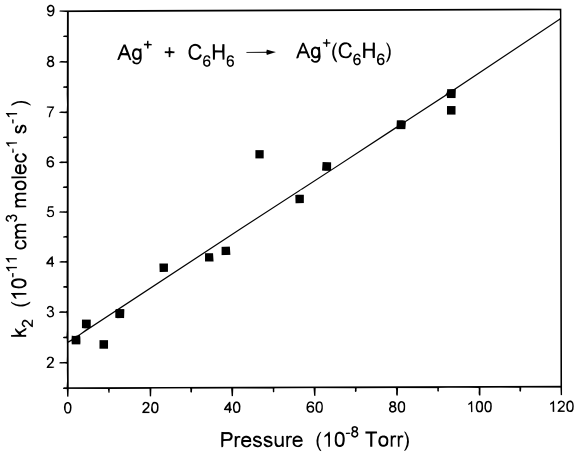

Figure 5. Apparent bimolecular association rate constants (k_{ra}) for the formation of $Ag^+(C_6H_6)$ complex as a function of pressure.

values corresponding to the midpoints of the convergence of the integrals in eq 9. In the case of Ag^+/benzene, k_r was also determined from the pressure dependence of the association rate constant plotted in Figure 5. The McMahon-type analysis which yields average values of k_b and k_r from the intercept and slope of such a plot is well-known[26,44] and was applied without complication in the present case. The radiative rate constant k_r found in this way was 16 s^{-1}. The MP2 based theoretical value of 10 s^{-1} for k_r is in reasonable agreement with this value. Multiplying the theoretical k_r values by a constant correction factor of 1.6 would lead to a 0.05 eV decrease in the modeling based estimated binding energy reported in Table 3 for Ag^+-(benzene).

Binding Energy. The radiative association rate constant as a function of binding energy was calculated employing eq 9 with the neutral pressure [L] set to zero. Fitting the experimental results to the theoretical values gives the corresponding binding energies. Figure 6 shows a plot of the predicted k_{ra} vs binding energy for the reaction of Ag^+ with C_6H_6, and it is clear that the experimental rate constant of 2.4×10^{-11} cm^3 $molecule^{-1}$ s^{-1} translates to a bond strength of 1.73 eV for this example. Since the experimental value is uncertain to perhaps a factor of 3 and the theoretical prediction is perhaps of similar uncertainty, an overall uncertainty of a factor of 5 for the rate constant fit seems realistic, translating to an uncertainty of about ±0.2 eV in binding energy. The binding energies derived from this

TABLE 3: Binding Energies from Detailed Modeling of RA Kinetics

	binding energy (E_0) (eV)	
complex	M^+L[a]	M^+L_2
Cd^+(benzene)	1.41 ± 0.2	
Ag^+(benzene)	1.73 ± 0.2 (1.39)[b]	1.50
Ag^+(isoprene)	1.70 ± 0.2 (1.59)	1.67
Ag^+(2-pentene)	(1.64)[c]	1.69
Ag^+(acetone)	1.66 ± 0.2 (1.49)	1.77
Ag^+(acetaldehyde)	[1.89 ± 0.2 (1.68)][d]	

[a] The primary values are obtained on the basis of the MP2 estimates for the frequencies and intensities while those in parentheses employ the HF estimates. [b] The value of 1.73 eV is lowered to 1.68 eV if the "experimental" value for k_r is used in place of the *ab initio*-derived value, as discussed in the text. [c] The MP2 estimate for this complex of 1.71 eV had to be corrected for the presence of one imaginary frequency as discussed in the Appendix. [d] See text for discussion of the doubtful significance of these numbers.

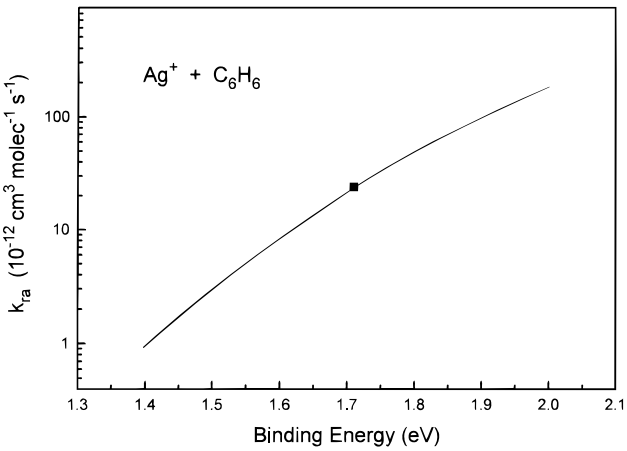

Figure 6. Plot of the predicted k_{ra} as a function of binding energy for the association of Ag^+ with C_6H_6. The square is the observed k_{ra}.

theoretical modeling of the observed association rate constants for all the reactions studied are summarized in Table 3. For comparative purposes the corresponding values obtained on the basis of the HF estimates, which have even greater uncertainties (perhaps ±0.4 eV), are also presented therein.

The procedure described above and applied to the M^+L complexes in Table 3 represents the best currently practicable approach to bond strength determination via RA kinetic analysis. Rates were also measured for formation of several Ag^+L_2 complexes. It was not feasible to analyze these by the same *ab initio* calculation-based procedure, but it seemed useful to make bond strength estimates for these by two more approximate approaches. One approach involved the simple estimation of the structures, frequencies, and absorption intensities from the *ab initio* data obtained for the monomer. In particular, the dimer structures were obtained by assuming that the Ag^+ center provides a center of inversion with the two ligands oriented equivalently to that of the monomer complex. The dimer frequencies were obtained by first assuming that each of the monomer frequencies were doubly degenerate. The required three additional frequencies for the dimer complex were then simply taken as the three frequencies of the monomer complex which had the greatest Ag^+ component. This last assumption is probably the most dubious as these three modes are most closely related to relative bending and torsional motions of the two ligands and are not necessarily related to the monomer modes. Estimated IR intensities were obtained in a similar fashion. The values obtained with this first approach are also reported in Table 3.

TABLE 4: Binding Energies from Standard Hydrocarbon Estimation of RA Kinetics

	binding energy (E_0) (eV)	
system	M^+L	M^+L_2
Cd^+/benzene	1.6 ± 0.3	
Ag^+/benzene	1.8 ± 0.3	1.8 ± 0.3
Ag^+/isoprene	1.8 ± 0.3	1.8 ± 0.3
Ag^+/2-pentene	1.6 ± 0.3	1.7 ± 0.3
Ag^+/acetone	1.8 ± 0.3	2.0 ± 0.3
Ag^+(acetaldehyde)	$(2.1 \pm 0.3)^a$	

[a] See text for discussion of the doubtful significance of this number.

The other approach involved the application of the "standard hydrocarbon" approach.[19,45−47] This semiquantitative estimation scheme is based on the principle that the properties of hydrocarbon-based systems which govern the RA kinetic behavior are reasonably predictable without detailed specification of the individual system of interest. This generic approach has had considerable success in modeling of a variety of radiative association systems[19] and appears to warrant reasonable semiquantitative confidence. Recently, a revision and recalculation of the standard hydrocarbon scheme was presented.[47] This revision has particular importance for the present work, since it incorporates for the first time a major variation in the predictions if one of the collision partners is an atom, as is the case in the present atomic ion reactions. Using this revised scheme, estimates of the bond strengths were made as shown in Table 4 for all of the complexes observed in this study. Our confidence in the usefulness of these predictions is strengthened by the observation that the standard hydrocarbon values for the M^+L species are in quite good agreement with the detailed modeling results in Table 3.

While both of these modeling procedures for the dimer complexes are clearly more uncertain than the procedure used for the monomer complexes, it is perhaps worth noting that the sensitivity is also slightly decreased in the dimer complex cases. In particular, an error of a factor of 2 in the rates typically correlates with only a 0.06 eV change in the estimated binding energy for the dimers as compared with a typical change of 0.08 eV for the monomers.

Temperature Dependence. For the present purpose, the temperature dependence is not necessary to our data analysis. However, it is interesting to see how the radiative association rate constant depends on the temperature and whether the kinetic modeling can be applied to the kinetic analysis of the radiative association process at temperatures higher than room temperature. Figure 7 shows the experimental and calculated association rate constants for the Ag^+/acetone reaction as a function of temperature ranging from 294 to 380 K.

Discussion

The present work has two interesting aspects. One is its exploration of the methodology, utility, accuracy, and convenience of the RA kinetics approach to bond strength determinations. The other is the actual bond strength results obtained for several previously unexamined or uncertain metal ion complexes. It will be clearest to discuss these aspects separately.

RA Kinetics Method. As illustrated in Figure 6 for the Ag^+-benzene association, the calculated radiative association rate constant (k_{ra}) is highly sensitive to the binding energy. In this case, when the binding energy varies by 0.1 eV, k_{ra} changes by more than a factor of 2. As a result, any inaccuracies in measuring k_{ra} yield only a relatively small error in the estimated binding energy. The major contribution to this sensitivity arises from the fact that the redissociation rate constant k_b decreases rapidly with increasing binding energy E_0.

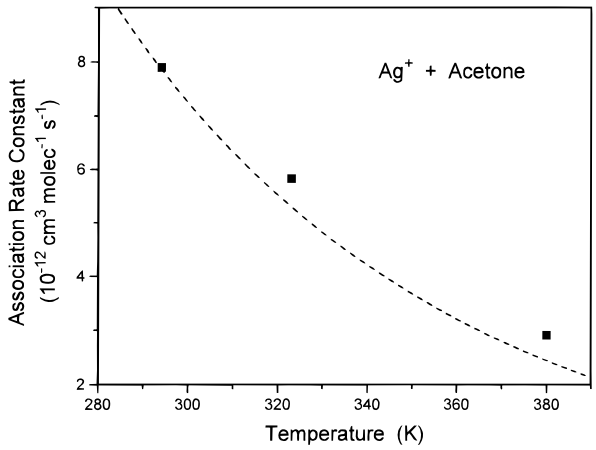

Figure 7. Temperature dependence of the association rate for Ag^+/acetone (squares show experimental points) compared with the theoretical prediction (dashed line). The fit of theory and experiment at 294 K is enforced by the choice of 1.65 eV for E_b.

TABLE 5: Binding Energies for Ag^+(Benzene)

E_0 (eV)	method	reference
1.58	*ab initio* calculation	48
≤1.31	photodissociation threshold	16
1.62 ± 0.07	threshold CID	9
$\leq 2.39 \pm 0.22$	photodissociation threshold	15
1.68 ± 0.2^a	present work	

[a] Taken as the average of the two MP2 values noted in Table 3, which differ according to the method chosen to assign k_r.

As discussed in ref 23, the temperature dependence of the RA kinetics has not thus far been found to be useful for directly determining bond strengths and was not used for that purpose in this study. However, it does provide a good check on the validity of the theoretical analysis which forms the basis for the bond strength assignments. Figure 7 shows the temperature dependence for the Ag^+/acetone association, which displays the expected strong decrease in stabilization efficiency with increasing temperature. Agreement with the theoretical expectation is not quite perfect but is entirely satisfactory within experimental uncertainty.

It is worth pointing out that the stabilization efficiency $\Phi(E,J)$ must not be too high if the association rate measurement is to be useful as an approach to obtaining E_0. When $\Phi(E,J)$ is too high (i.e., approaching unity), nearly every collision of the reactant pair forms an association product, and only a lower limit of E_0 can be derived from the association rate constant. If $\Phi(E,J)$ is inconveniently high for a given system, an increase in operating temperature may bring it down to an appropriate range. As shown in the present work for the Ag^+/acetone example, the RA kinetics analysis gives a good representation of the temperature dependence and can be used to find bond strengths at whatever temperature is operationally convenient.

Bond Strength Values. Among the binding energies determined here, $Ag^+-(C_6H_6)$ has been measured and calculated previously by several different approaches, and an upper limit has been assigned to Ag^+-(acetone) from photodissociation threshold observations.[16] Table 5 lists the binding energies for $Ag^+-(C_6H_6)$ determined by various methods. The value in the present work agrees well with the theoretical value[48] and the CID threshold result[9] and is consistent with the generous upper limit of 2.39 eV from photodissociation reported by Freiser's group.[15] The upper limit of binding energy reported by

Duncan's group from charge-transfer photodissociation[16] seems to be too low.

Duncan and co-workers also derived an upper limit of 1.34 eV on the binding energy of Ag^+(acetone) from the charge-transfer photodissociation threshold.[16] This number is lower than the present value of 1.66 eV by an amount which is probably outside the uncertainties of the techniques. Given our present understanding of RA kinetics, it is not credible that the binding energy could be as low as 1.34 eV and still give observable radiative association at room temperature for this system, so we believe the value from Duncan *et al.* is unreasonably low.

The charge-transfer photodissociation thresholds measured by Duncan's group[16] for $Ag^+(C_6H_6)$ and Ag^+(acetone) might be expected to give good upper limits to the bond strengths, but in fact they appear to be low. For $Ag^+(C_6H_6)$ in particular, results from assorted techniques shown in Table 5 suggest quite strongly that this bond strength is not less than about 1.5 eV, and probably higher, which is clearly not consistent with Willey *et al.* Two possible complications of photodissociation threshold measurements may have acted to give incorrectly low thresholds. First, as pointed out by these authors, the internal energy of the parent ions may have been significant. While the ions were jet cooled before extraction, helium collisions are not efficient in thermalizing vibrational and electronic excitation, and a fraction of the parent ion population might have retained sufficient internal energy to move the observed threshold by a few tenths of an electronvolt. Second, two-photon photodissociation might have made a contribution in the threshold region. While Willey *et al.* were careful to verify linear dependence of the dissociation on light intensity, nevertheless the photodissociation kinetic behavior at low extent of dissociation can appear to follow one-photon characteristics even if there are a substantial fraction of two-photon ions in the population.[49,50] With these two possibilities in mind, it seems most reasonable to conclude that their observed thresholds were actually a few tenths of an electronvolt below the true, 0 K one-photon thresholds.

The binding of Ag^+ to ethylene makes an interesting comparison with the present result for pentene. Although the ethylene complex is not accessible to RA kinetic study (the association efficiency per collision at room temperature is expected to be less than 10^{-7}), comparison is possible with the value of 1.47 eV found by Guo and Castleman[51] using high-pressure equilibrium techniques. The present value of 1.71 eV for pentene binding is larger than this by an amount which is readily ascribed to the slightly increased electrostatic binding to the more polarizable pentene molecule. It thus appears that the chemical (i.e., nonelectrostatic) component of the binding, which Guo and Castleman considered to be substantial in the ethylene case, is similar in the pentene case. We can conclude that the nature of Ag^+ binding to the double bond is probably similar in the ethylene and pentene cases.

From Tables 3 and 4 it is seen that the binding energies for the first and second ligands are the same within experimental and modeling error in each case of a ligand complexing with Ag^+.[52] Similarly, Guo and Castleman found the first and second ligand binding energies to be very similar for ethylene binding to Ag^+. It seems to be general that Ag^+ binds two π ligands equally well with little mutual interaction, at least as reflected in the binding energies. The fact that no binding of a third ligand was observed (discounting the anomalous acetaldehyde case) indicates that the binding to such a possible third ligand is much weaker, certainly not stronger than about 1 eV.

It is notable that Ag^+ binds to these various ligands with quite similar binding energies (near 1.7 eV). This probably reflects to a considerable degree the fact that a large fraction of the binding in these complexes is electrostatic, which will be similar for sets of ligands, like these, whose polarizabilities are not very different. The specific variations in the Ag^+ interactions with the various π or n electrons of these ligands may be relatively small and not discernible outside the measurement uncertainties.

Acetaldehyde. The acetaldehyde results are anomalous in two respects. First, the binding energy derived from the RA kinetics analysis is unreasonably high compared with the other values shown in Table 3. Put another way, the small number of degrees of freedom of the Ag^+/acetaldehyde complex means that the association rate should be unobservably slow if the binding energy is comparable to similar systems (in particular Ag^+/acetone). Strengthening this idea, the present *ab initio* calculations of the bond strength have given no indication that this bond strength should be higher than other comparable π ligands. The second anomaly is that this is the only reactant so far observed that adds more than two monomer units to Ag^+.

It may be that the apparent strong binding and extensive clustering in the acetaldehyde case reflect binding which is actually several tenths of an electronvolt stronger than for the olefins and acetone, although this would seem intuitively surprising, and is not supported by the *ab initio* results. Another possible explanation of these anomalies is that Ag^+ initiates an exothermic rearrangement and/or bond-insertion process with acetaldehyde, resulting in an effective complexation energy several tenths of an electronvolt higher than the simple π complexation energy. Such a process could explain the unexpectedly rapid radiative association reaction and also could be imagined to initiate a silver ion-catalyzed polymerization of acetaldehyde, resulting in sequential addition of an indefinite number of monomer units. However, any plausible exothermic addition reaction of acetaldehyde to Ag^+ giving a more stable $AgC_2H_4O^+$ product than the simple π complex would be likely to further dissociate to a lower mass Ag^+L species, and we see no evidence for such species.

Another possibility is that the modeling is exceptionally inaccurate in this case, perhaps due to exceptionally large anharmonic effects. Such a possibility is plausible since the small size of the ligand leads to an average energy per mode which is somewhat greater than for the other ligands. However, detailed evaluations employing direct *ab initio* evaluation of phase space integrals suggest that the anharmonic contributions due to the intermolecular modes of the complex are negligible.[53] It is still possible that inaccurate treatments of the torsional modes are responsible for the unexpected results. However, sample evaluations also suggest that such corrections would be quite minor.

Overall, it seems most likely that the observed reaction with Ag^+ is not that of acetaldehyde monomer, but rather reflects reaction of a small polymeric impurity in the neutral acetaldehyde vapor, presumably dimer, trimer, or tetramer. Although the sample was clean by NMR, a polymeric contaminant of the order of 0.02% could not be ruled out; if such an impurity were to undergo a bimolecular reaction with Ag^+ at close to the collision rate, it could appear as if acetaldehyde monomer were adding at the low apparent rate constant given in Table 1. This explanation would invalidate the RA kinetics analysis used above to derive the Ag^+(acetaldehyde) bond strength, and accordingly we consider that the values given for this particular bond strength in Tables 2 and 3 may well be meaningless. Similarly, the formation of higher clusters shown in Figure 4 is interesting, but since the identity of the molecule adding to the cluster is uncertain, it is futile to try to interpret these observations.

MP2- versus HF-Based Modeling. The close similarity between the binding energies calculated *ab initio* at the MP2 level and those obtained on the basis of the modeling at the MP2 level (for all but the anomalous acetaldehyde case) provides further confidence in the basic validity of the present binding estimates. In particular, the more accurate the *ab initio* estimated binding energy is the greater the confidence one may have in the corresponding *ab initio* estimates for the spectroscopic properties and thereby in the modeling. At the HF level the purely *ab initio* estimated binding energies are generally much lower than the modeling-based results. Notably, however, the modeling-based results employing the HF spectroscopic properties are in greatly improved agreement with those obtained on the basis of the modeling at the MP2 level, with a large discrepancy occurring only for Ag^+/benzene. Thus, even when the purely *ab initio* estimates for the binding energy are quite inaccurate, one can still obtain quite reasonable estimates for the binding energies by combining *ab initio* results with modeling of experimental RA kinetics data. The very poor HF/modeling result for Ag^+/benzene, tracing back to the obviously unreasonable 11 cm^{-1} normal mode generated by the HF level of calculation, reinforces the point that the thoughtless use of unreasonable low-level *ab initio* results in this context is worse than useless.

The discrepancy for the Ag^+/benzene complex arises primarily because of an apparently incorrect reduction in symmetry at the HF level to C_s symmetry, which ultimately results in an unbelievably low bending frequency of 11 cm^{-1}. As a result, the harmonic state density estimate at the HF level likely greatly overestimates the true state density at the HF level, and improved estimates of the HF state density employing anharmonic corrections might be expected to provide more reasonable results for the binding energy. The small underestimates seen at the HF level for the other cases are due to lower estimates for both the metal−ligand frequencies and the average radiative intensities and give an indication of the sensitivity of the modeling to the level of accuracy of the underlying quantum chemical data.

Conclusions

The binding energies of metal ion−ligand complexes were measured from the analysis of association reaction kinetics. The strong dependence of the redissociation rate constant on binding energy allows accurate determination of binding energies of the metal ion−ligand complexes. The binding energies for cadmium ion/benzene and several silver ion complexes are summarized in Table 3.

The recently developed approach to RA kinetic modeling, based on a canonical average over energy- and angular momentum-resolved rate constants derived from transition state theory, provides a satisfactory framework for analysis of experimental results. The binding energy of 1.68 eV for $Ag^+(C_6H_6)$ derived from the observed association rate constant employing the present kinetic modeling supports the preponderance of previous information suggesting a bond energy falling in the vicinity of 1.6−1.7 eV. For the other complexes, where the binding energies were not previously known, the binding energy measurements from this study are expected to be as good as the $Ag^+(C_6H_6)$ result. Kinetic analysis of radiative association reactions has the promise of becoming a generally useful approach to measuring binding energies of association complexes.

Acknowledgment. The support of the donors of the Petroleum Research Fund, administered by the American Chemical Society, is gratefully acknowledged, as is the provision of computational support through the Ohio Supercomputer Center for some parts of the quantum chemical aspects of this work. The support of the National Science Foundation is acknowledged (through Grant CHE-9423725 and through partial support of Y.-P.H. by NSF funds administered by the NHMFL). We are grateful to Prof. Alan Marshall for the use of instrumentation in his laboratory at the NHMFL.

TABLE 6: MP2 Frequencies of the Three Vibrational Modes of Each ML^+ Complex with the Largest Components of Metal Atom Movement

species	frequencies (cm^{-1}) MP2	HF
Cd^+(benzene)	150, 35, 35	
Ag^+(benzene)	160, 42, 42	154, 42, 11
Ag^+(isoprene)	284, 113, 52	197, 70, 55
Ag^+(2-pentene)	123, 94, −65	133, 87, 79
Ag^+(acetone)	220, 84, 69	183, 89, 28
Ag^+(acetaldehyde)	217, 95, 94	192, 85, 60

TABLE 7: Equilibrium M^+ Ligand Bond Lengths (Å) and Bond Angles (deg)

species	bond length[a]	bond angle[a]
Cd^+(benzene)	Cd−ring center 2.44	
Ag^+(benzene)	Ag−ring center 2.27 (2.56)	
Ag^+(isoprene)	Ag−C_1 2.35 (2.48) Ag−C_2 2.50(2.76)	C_1AgC_2 33 (29)
Ag^+(2-pentene)	Ag−C_2 2.40 (2.59) Ag−C_3 2.42(2.59)	C_2AgC_3 33 (30)
Ag^+(acetone)	AgO 2.22 (2.27)	AgOC 141 (165)
Ag^+(acetaldehyde)	AgO 2.24 (2.30)	AgOC 142 (158)

[a] The primary results are the MP2 values while those in parentheses are the HF results.

TABLE 8: Rotational Constants, Symmetry Numbers, Polarizabilities, and Dipole Moments for the Ligands

species	*A*, *B*, *C* (cm^{-1})	σ	α ($Å^3$)	μ (D)
benzene	0.19, 0.19, 0.096	12	10.6	0
isoprene	0.28, 0.14, 0.095	1	10	0.25
2-pentene	0.56, 0.070, 0.068	1	9.8	0.5
acetone	0.33, 0.28, 0.16	2	6.4	2.9
acetaldehyde	1.88, 0.34, 0.30	1	4.6	2.8

Appendix

The full set of molecular data used in the RRKM calculations consists of the rotational constants, polarizabilities, dipole moments, and symmetry numbers, along with the vibrational frequencies and infrared intensities, for each of the ligands and the complexes. The full set of vibrational frequencies and IR intensities are tabulated and discussed in the Supporting Information. The overall modeling is most sensitive to the estimated frequencies for the metal−ligand modes, so for more convenient reference the HF and MP2 results for this subset of frequencies are summarized in Table 6. The main burden of this appendix is to summarize the molecular constants, given in Tables 7−9, and to discuss the assignment of the symmetry numbers for these systems.

Discussion of symmetry and related effects in these systems seems appropriate, since such symmetry considerations are often neither straightforward nor unimportant for such systems. The various numbers of states, densities of states, and partition

TABLE 9: Rotational Constants and Effective Symmetry Numbers for the Monomer and Dimer Complexes

species	*A*, *B*, *C* (cm^{-1}) monomer	σ	*A*, *B*, *C* (cm^{-1}) dimer	σ
Cd^+(benzene)	0.090, 0.046, 0.046	6		
Ag^+(benzene)	0.093, 0.052, 0.052	6	0.047, 0.017, 0.017	12
Ag^+(isoprene)	0.13, 0.038, 0.036	0.5	0.058, 0.014, 0.013	0.5
Ag^+(2-pentene)	0.093, 0.037, 0.028	1	0.046, 0.014, 0.011	2
Ag^+(acetone)	0.29, 0.036, 0.032	1	0.15, 0.012, 0.011	2
Ag^+(acetaldehyde)	1.84, 0.042, 0.041	0.5		

functions properly include rotational symmetry numbers. Such symmetry numbers are generally well defined and correctly reproduce typical reaction path degeneracies. However, for the present associations there are a number of instances where there are near degeneracies for the binding sites of the ligands which can only be handled with special considerations. In particular, for the association of acetaldehyde the Ag^+ may bind to either the methyl or H atom sides of the CO bond. At the MP2 level the difference in binding energy between these two sites is only 183 cm^{-1}. For such a small difference in binding energy one might expect the total density of states for the complex to be effectively double that estimated from a rigid rotor harmonic oscillator estimate for the single lowest binding site. This factor of 2 increase in the density of states was explicitly included here via the assignment of an effective symmetry number of $^1/_2$ for the complex.

For acetone there are again two separate binding sites. However, these two binding sites are exactly related by symmetry and so the inclusion of the rotational symmetry number of two for acetone, and also for the transition state, properly incorporates this degeneracy. Similarly, for benzene in C_{6v} symmetry the rotational symmetries take proper account of all reaction path and binding site degeneracies and near degeneracies.

For 2-pentene there is only one binding site. However, there are multiple forms of pentene and one should really evaluate how the contributions from each of these forms change during the progression from reactants to complex. For example, there are both cis and trans isomers of 2-pentene, and there are also numerous other isomers of C_5H_{10} such as 1-pentene, cyclopentane, and 2-methyl-2-butene. Also, 2-pentene is not even the most stable form of C_5H_{10}. Each of these isomers may contribute differently to the reactant and complex partition functions. For example, the reactant likely samples only the cis and trans forms of 2-pentene. In contrast, the complex, due to the additional available energy, may sample some other forms depending on the barrier to interconversion among the isomers. In the absence of any information regarding the distribution of isomers in the complex we have assumed here that only *cis*- and *trans*-2-pentene are accessed.

For isoprene the Ag^+ species may bind to either one of the two C═C bonds. At the MP2 level the difference in energetics is estimated to be only 105 cm^{-1}. Thus, an effective symmetry number of $^1/_2$ was employed for the complex in order to provide a doubling of the effective density of states for the complex.

At the MP2 level the optimized structure for the Ag^+ benzene complex is of C_{6v} symmetry, which presents no complications in the modeling. However, at the HF level it is only of C_s symmetry, and the estimated bending frequency has a remarkably low value of only 11 cm^{-1}. Overall, this variation of symmetry from the HF to the MP2 level suggests that the potential energy surface for the Ag^+−benzene interaction is likely highly anharmonic and that the accurate estimation of the density of states may be difficult. In any case, the HF estimates almost certainly overestimate the true density, and thus the corresponding estimated binding energy should be taken as a lower bound. Indeed, assuming that the HF structure is actually of C_{6v} symmetry yields an estimate for the binding energy of 1.55 eV, which seems much more reasonable.

Similar considerations were employed in the generation of the effective symmetry numbers for the dimer complexes and will not be reiterated here.

One of the greatest uncertainties in the modeling regards the treatment of the torsional modes of the ligands. A harmonic treatment for these modes is not expected to be completely accurate. However, one may hope that the inaccuracies in their treatment are roughly canceled in taking the ratios of their contributions to the reactants and complexes. This may not be entirely correct since the effective temperature of the complex is considerably greater than that of the reactants. Furthermore, the presence of the metal ion may dramatically change the relative energetics of the different local torsional minima. For the most part the consideration of such effects was deemed to be too involved for the present study. However, some limited quantum chemical investigations were performed. In particular, it was found that rotation of the methyl group by 180° led to an increase in energy of 368 and 366 cm^{-1} for acetaldehye and Ag^+(acetaldehyde), respectively. This suggests that at least the Ag^+ does not introduce great changes in the torsional potential for this species. For 2-pentene similar results were obtained for a cis to trans rotation. However, for isoprene the cis to trans energy difference changes from 832 to 545 cm^{-1} with the addition of the Ag^+ species.

The primary structural data corresponding to a metal to ligand bond length and bond angle are summarized in Table 7 for each of the complexes. The molecular symmetry was found to be C_1 for all but the acetaldehye (C_s) and benzene complexes. Even the acetone complex is of C_1 symmetry due to a minor out-of-plane feature of the bonding. The metal−ligand bond lengths are calculated to be greater at the HF level by amounts ranging from 0.05 to 0.29 Å, with the discrepancy increasing with increasing number of π bonds, which also correlates well with the deviation in purely *ab initio* binding energies. The bond angles show an exceptionally large variation of 15° for the AgOC bond angles in the acetone and acetaldehyde complexes.

The optimized Cartesian coordinates for the molecular structures of each of the complexes and reactants are available from the authors upon request. Rather than the full molecular structures, the kinetic modeling actually requires only rotational constants for each of the reactants and the complex. MP2 estimates of these are provided in Tables 8 and 9 for all of the reactants and complexes, as well as the more approximately estimated values for the dimer complexes. Also reported there are the molecular polarizabilities, dipole moments, and rotational symmetry numbers. The symmetry numbers for the transition states are taken to be equivalent to the product of those for the free reactants.

Supporting Information Available: Tables S1−S6 of the vibrational frequencies and IR intensities evaluated at the MP2 and HF levels for Ag^+ and Cd^+ complexes (11 pages). Ordering information is given on any current masthead page.

References and Notes

(1) Martinho-Simhoes, J. A.; Beauchamp, J. L. *Chem. Rev.* **1990**, *90*, 629.

(2) Russell, D. H. *Gas-Phase Inorganic Chemistry*; Plenum Press: New York, 1989.

(3) Freiser, B. S. *Acc. Chem. Res.* **1994**, *27*, 353.

(4) Freiser, B. S. *J. Mass Spectrom.* **1996**, *31*, 703.

(5) Uppal, J. S.; Staley, R. H. *J. Am. Chem. Soc.* **1982**, *104*, 1235.

(6) Schröder, D.; Hrušák, J.; Hertwig, R. H.; Koch, W.; Schwerdtfeger, P.; Schwarz, H. *Organometallics* **1995**, *14*, 312.

(7) Van Koppen, P. A. M.; Jacobson, D. B.; Illies, A.; Bowers, M. T.; Hanratty, M.; Beauchamp, J. L. *J. Am. Chem. Soc.* **1989**, *111*, 1991.
(8) Schultz, R. H.; Armentrout, P. B. *J. Phys. Chem.* **1993**, *97*, 596.
(9) Chen, Y. M.; Armentrout, P. B. *Chem. Phys. Lett.* **1993**, *210*, 123.
(10) Meyer, F.; Khan, F. A.; Armentrout, P. B. *J. Am. Chem. Soc.* **1995**, *117*, 9740.
(11) Cooks, R. G.; Patrick, J. S.; Kotiaho, T.; McLuckey, S. A. *Mass Spectrom. Rev.* **1994**, *13*, 287.
(12) Cerda, B. A.; Wesdemiotis, C. *J. Am. Chem. Soc.* **1995**, *117*, 9734.
(13) Sallans, L.; Laude, D. R.; Freiser, B. S. *J. Am. Chem. Soc.* **1989**, *111*, 865.
(14) van der Hart, W. J. *Mass Spectrom. Rev.* **1989**, *8*, 237.
(15) Afzaal, S.; Freiser, B. S. *Chem. Phys. Lett.* **1994**, *218*, 254.
(16) Willey, K. F.; Cheng, P. Y.; Bishop, M. B.; Duncan, M. A. *J. Am. Chem. Soc.* **1991**, *113*, 4721.
(17) Faulk, J. D.; Dunbar, R. C. *J. Am. Chem. Soc.* **1992**, *114*, 8596.
(18) Dunbar, R. C.; Uechi, G. T.; Solooki, D.; Tessier, C. A.; Youngs, W.; Asamoto, B. *J. Am. Chem. Soc.* **1993**, *115*, 12477.
(19) Dunbar, R. C. Ion-Molecule Radiative Association. In *Current Topics in Ion Chemistry and Physics*; Ng, C. Y., Baer, T., Powis, I., Eds.; Wiley: New York, 1994; Vol. II.
(20) Weddle, G. H.; Dunbar, R. C. *Int. J. Mass Spectrom. Ion Processes* **1994**, *134*, 73.
(21) Cheng, Y. W.; Dunbar, R. C. *J. Phys. Chem.* **1995**, *99*, 10802.
(22) Dunbar, R. C.; Klippenstein, S. J.; Hrušák, J.; Stöckigt, D.; Schwarz, H. *J. Am. Chem. Soc.* **1996**, *118*, 5277.
(23) Klippenstein, S. J.; Yang, Y.-C.; Ryzhov, V.; Dunbar, R. C. *J. Chem. Phys.* **1996**, *104*, 4502.
(24) van der Hart, W. J.; van Sprang, H. A. *J. Am. Chem. Soc.* **1977**, *99*, 32.
(25) Bartmess, J. E.; Georgiadis, R. M. *Vacuum* **1983**, *33*, 149.
(26) Kofel, P.; McMahon, T. B. *J. Phys. Chem.* **1988**, *92*, 617.
(27) Dunbar, R. C. *Mass Spectrom. Rev.* **1992**, *11*, 309.
(28) Dunbar, R. C. *J. Chem. Phys.* **1989**, *90*, 7369.
(29) Ho, Y.-P.; Yang, Y.-C.; Klippenstein, S. J.; Dunbar, R. C. *J. Phys. Chem.* **1995**, *99*, 12115.
(30) Thölmann, D.; McCormick, A.; McMahon, T. B. *J. Phys. Chem.* **1994**, *98*, 1156.
(31) Dunbar, R. C. *Spectrochim. Acta* **1975**, *31A*, 797.
(32) GAUSSIAN 92/DFT: Frisch, M. J.; Trucks, G. W.; Schlegel, H. B.; Gill, P. M. W.; Johnson, B. G.; Wong, M. W.; Foresman, J. B.; Robb, M. A.; Head-Gordon, M.; Replogle, E. S.; Gomperts, R.; Andres, J. L.; Raghavachari, K.; Binkley, J. S.; Gonzalez, C.; Martin, R. L.; Fox, D. J.; Defrees, D. J.; Baker, J.; Stewart, J. J. P.; Pople, J. A., Gaussian, Inc., Pittsburgh, PA, 1993.
(33) GAUSSIAN 94: Frisch, M. J.; Trucks, G. W.; Schlegel, H. B.; Gill, P. M. W.; Johnson, B. G.; Robb, M. A.; Cheeseman, J. R.; Keith, T. A.; Petersson, G. A.; Montgomery, J. A.; Raghavachari, K.; Al-Laham, M. A.; Zakrzewski, V. G.; Ortiz, J. V.; Foresman, J. B.; Cioslowski, J.; Stefanov, B. B.; Nanyakkara, A.; Challacombe, M.; Peng, C. Y.; Ayala, P. Y.; Chen, W.; Wong, M. W.; Andres, J. L.; Replogle, E. S.; Gomperts, R.; Martin, R. L.; Fox, D. J.; Binkley, J. S.; Defrees, D. J.; Baker, J.; Stewart, J. J. P.; Head-Gordon, M.; Gonzalez, C.; Pople, J. A., Gaussian, Inc., Pittsburgh, PA, 1995.
(34) Hehre, W. J.; Radom, L.; Schleyer, P. v. R.; Pople, J. A. *Ab Initio Molecular Orbital Theory*; Wiley: New York, 1986.
(35) Langhoff, S. R.; Pettersson, L. G. M.; Bauschlicher, C. W.; Partridge, H. *J. Chem. Phys.* **1987**, *86*, 268.
(36) Hay, P. J.; Wadt, W. R. *J. Chem. Phys.* **1985**, *82*, 299.
(37) Dunning, T. H.; Hay, P. J. In *Modern Theoretical Chemistry*; Schaeffer, H. F., Ed.; Plenum: New York, 1976.
(38) Roothan, C. C. J. *Rev. Mod. Phys.* **1951**, *23*, 69.
(39) Moller, C.; Plesset, M. S. *Phys. Rev.* **1934**, *46*, 618.
(40) Pople, J. A.; Binkley, J. S.; Seeger, R. *Int. J. Quantum Chem. Symp.* **1976**, *10*, 1.
(41) Yamaguchi, Y.; Frisch, M.; Gaw, H. F.; Binkley, J. S. *J. Chem. Phys.* **1986**, *84*, 2262.
(42) Stanton, J. F.; Watts, J. D.; Bartlett, R. J. *J. Chem. Phys.* **1991**, *94*, 404.
(43) Becke, A. D. *J. Chem. Phys.* **1993**, *98*, 5648.
(44) Fisher, J. J.; McMahon, T. B. *Int. J. Mass Spectrom. Ion Processes* **1990**, *100*, 701.
(45) Dunbar, R. C. *Int. J. Mass Spectrom. Ion Processes* **1990**, *100*, 701.
(46) Herbst, E.; Dunbar, R. C. *Mon. Not. R. Astron. Soc.* **1991**, *253*, 341.
(47) Dunbar, R. C. *Int. J. Mass Spectrom. Ion Processes*, in press.
(48) Bauschlicher, C. W., Jr.; Partridge, H.; Langhoff, S. R. *J. Phys. Chem.* **1992**, *96*, 3273.
(49) van Velzen, P. N. T.; van der Hart, W. J. *Chem. Phys.* **1981**, *61*, 335.
(50) Dunbar, R. C.; Honovich, J. P. *Int. J. Mass Spectrom. Ion Processes* **1984**, *58*, 25.
(51) Guo, B. C.; A. W. Castleman, J. *Chem. Phys. Lett.* **1991**, *181*, 16.
(52) The low binding energy estimated for $Ag^+(benzene)_2$ in Table 3 from the approximate modeling approach is an apparent exception to this generalization, although the quoted uncertainties are large enough to make this deviation statistically insignificant. This binding energy number is somewhat lower than the value estimated by the standard hydrocarbon model in Table 4 and is also lower than the estimates for the other systems. The lowness of this value compared with the standard hydrocarbon model can be traced primarily to symmetry number considerations which are only incorporated in an average fashion in the latter approach. There is in fact some uncertainty about the numerical validity of the particular summetry corrections adopted. In sum, we would put little stock in these differences in binding energies since they are within the quoted uncertainties and may well be simply an indication of the limits of confidence of the modeling.
(53) Klippenstein, S. J., unpublished results.
(54) *Handbook of Chemistry and Physics*, 74th ed.; CRC Press: Cleveland, 1993.